Electronic Supplementary Material (ESI) for Nanoscale Advances.

Supporting Information

Clearance of single-wall carbon nanotubes from the mouse lung: a quantitative evaluation

Minfang Zhang[a], Ying Xu[a], Mei Yang[a], Masako Yudasaka [b,c], Toshiya Okazaki[a]*

[a]CNT-Application Research Center, National Institute of Advanced Science and Technology (AIST), 1-1-1 Higashi, Tsukuba, Ibaraki 305-8565, Japan.
[b]Research Institute of Nanomaterials, National Institute of Advanced Science and Technology (AIST), 1-1-1 Higashi, Tsukuba, Ibaraki 305-8565, Japan.
[c]Faculty of Science & Technology, Meijo University. 1-501 Shiogamaguchi, Tenpaku-ku, Nagoya 468-8502, Japan,

Figure SI-1

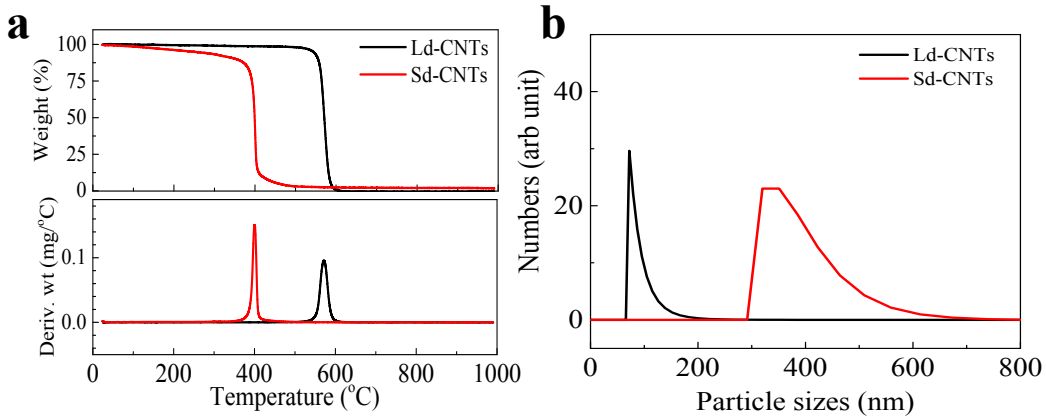

Figure SI-1. Characteristics of large-diameter carbon nanotubes (Ld-CNTs) and small-diameter carbon nanotubes (Sd-CNTs). (a)TGA results of Ld-CNTs and Sd-CNTs for weight change (up) and derivative weight change per temperature (below); (b) The dynamic light scattering (DLS) measurement results for Ld-CNTs and Sd-CNTs dispersions.

Figure SI-2

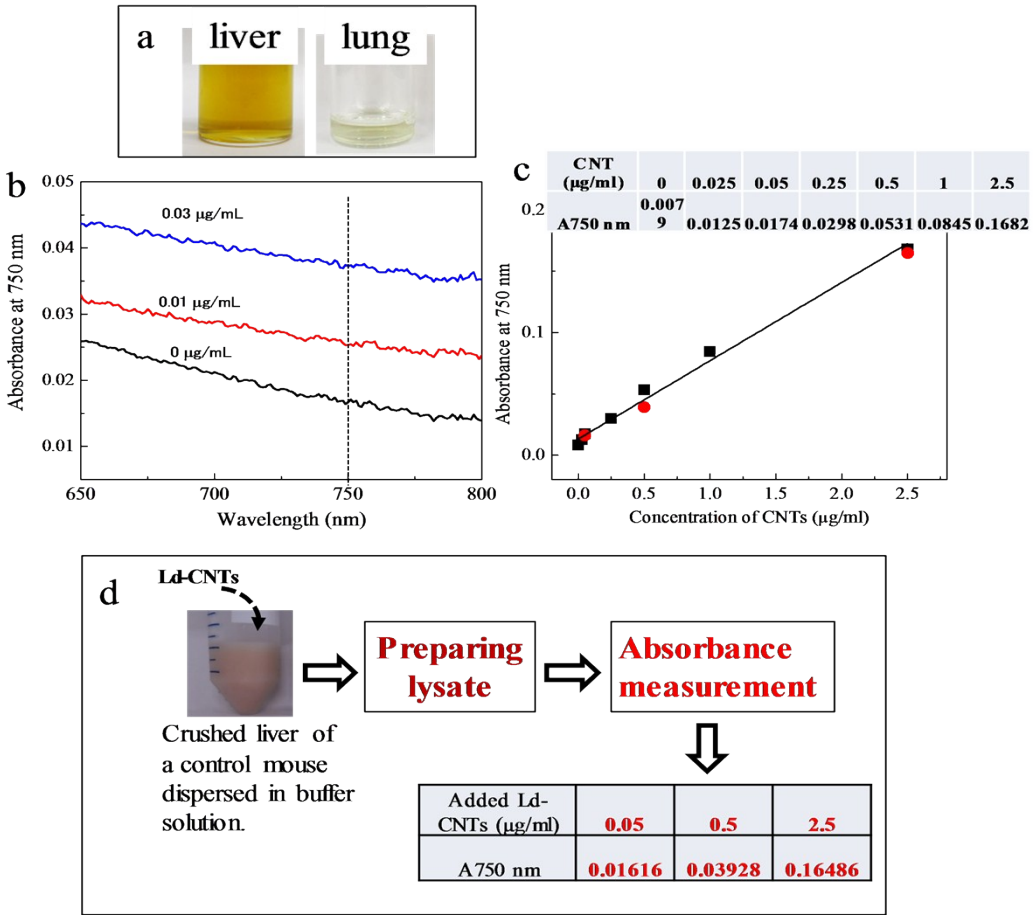

Figure SI-2. (a) Images of representative lung and liver lysates, showing that the lysates were transparent. (b) The light absorption spectra of lung lysates spiked with large-diameter carbon nanotubes (Ld-CNTs) to concentrations of 0, 0.01, and 0.03 μg/mL. (c) A calibration line was generated based on the absorbances in (b). (d) Protocol for testing the accuracy of the near infrared (NIR) light absorption method. Here, the Ld-CNTs were added into a crushed liver dispersion at concentrations of 0.05, 0.5, and 2.5 μg/mL, and the lysing procedure was performed. The absorbances at 750 nm of the three samples were 0.01616, 0.03928, and 0.16486, which was equivalent to the concentrations obtained using the calibration line (b, red circle).

Figure SI-3

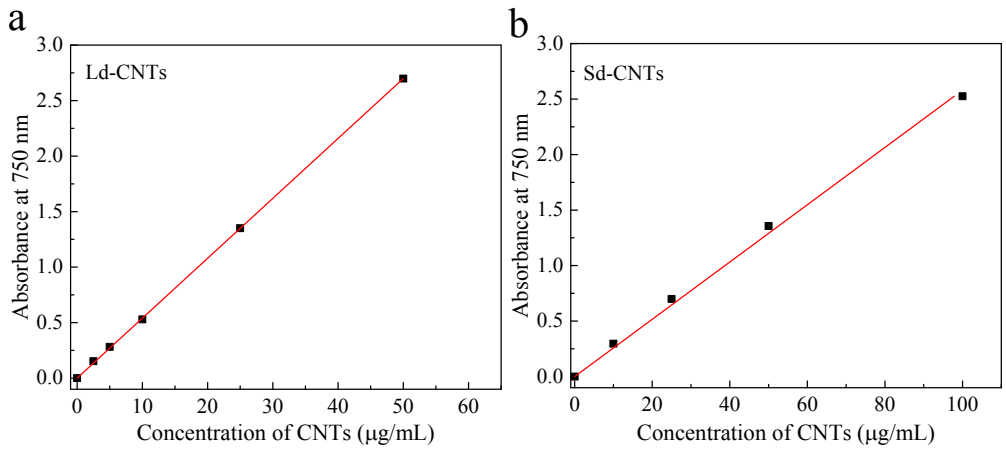

Figure SI-3. Calibration curves of large-diameter carbon nanotubes (Ld-CNTs) (a) or small-diameter carbon nanotubes (Sd-CNTs) (b).

Figure SI-4

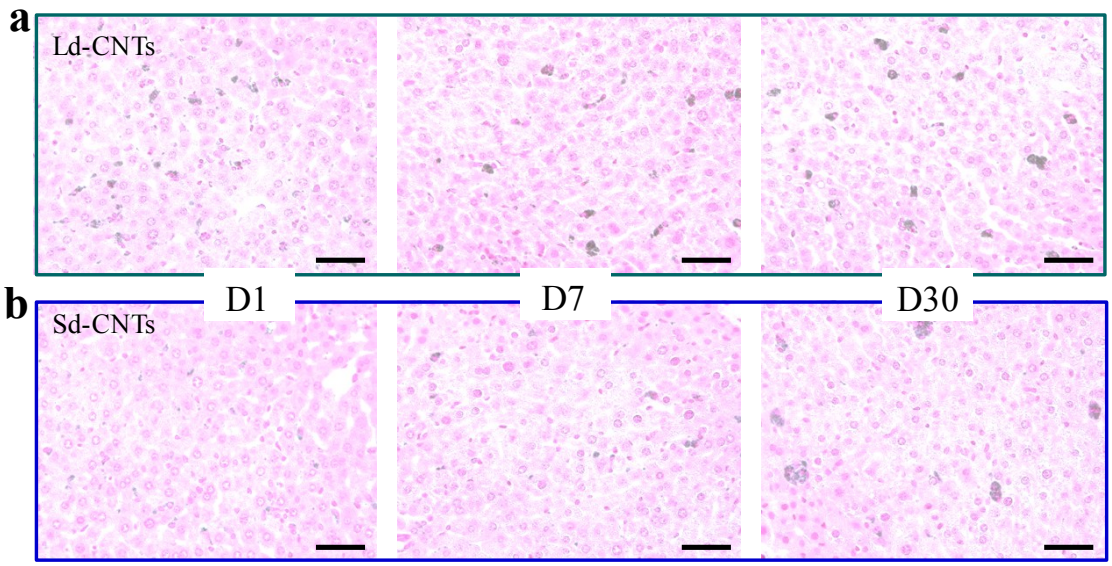

Figure SI-4. Optical microscopy images of nuclear fast red solution (kernechtrot) stained mouse liver tissues harvested at days (D)1, D7, and D30 after intravenous administration of a single dose of large-diameter carbon nanotubes (Ld-CNTs) (a) or small-diameter carbon nanotubes (Sd-CNTs) (b). The Ld-CNTs and Sd-CNTs as shown as black spots seemed to accumulate in the Kupffer cells, and Ld-CNTs were more visible. Scale bar: 50 μm.

Figure SI-5

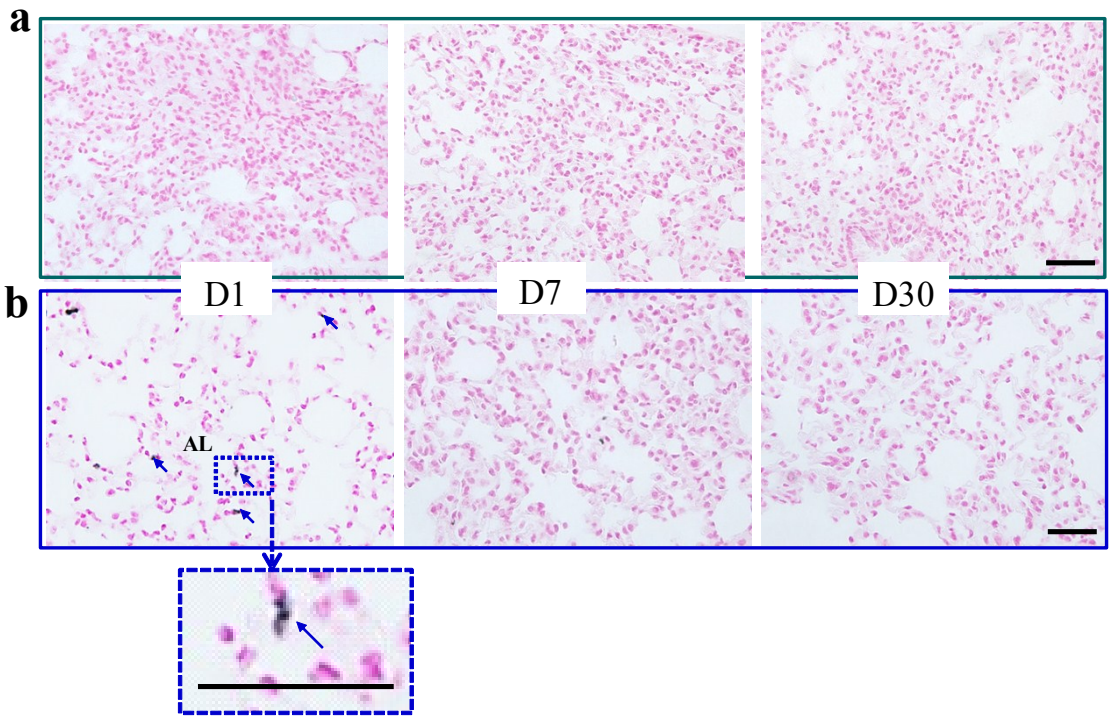

Figure SI-5. Optical microscopy images of nuclear fast red solution (kernechtrot) stained mouse lung tissues harvested at days (D)1, D7, and D30 after intravenous administration of a single dose of large-diameter carbon nanotubes (Ld-CNTs) (a) or small-diameter carbon nanotubes (Sd-CNTs) (b). The Ld-CNTs in the lung ware difficult to identify. The Sd-CNTs, which appear as black dots, seemed to accumulate inside the alveolar macrophages (arrows; the magnified image is from a mouse injected with Sd-CNTs, D1). Scale bar: 50 μm.

Figure SI-6

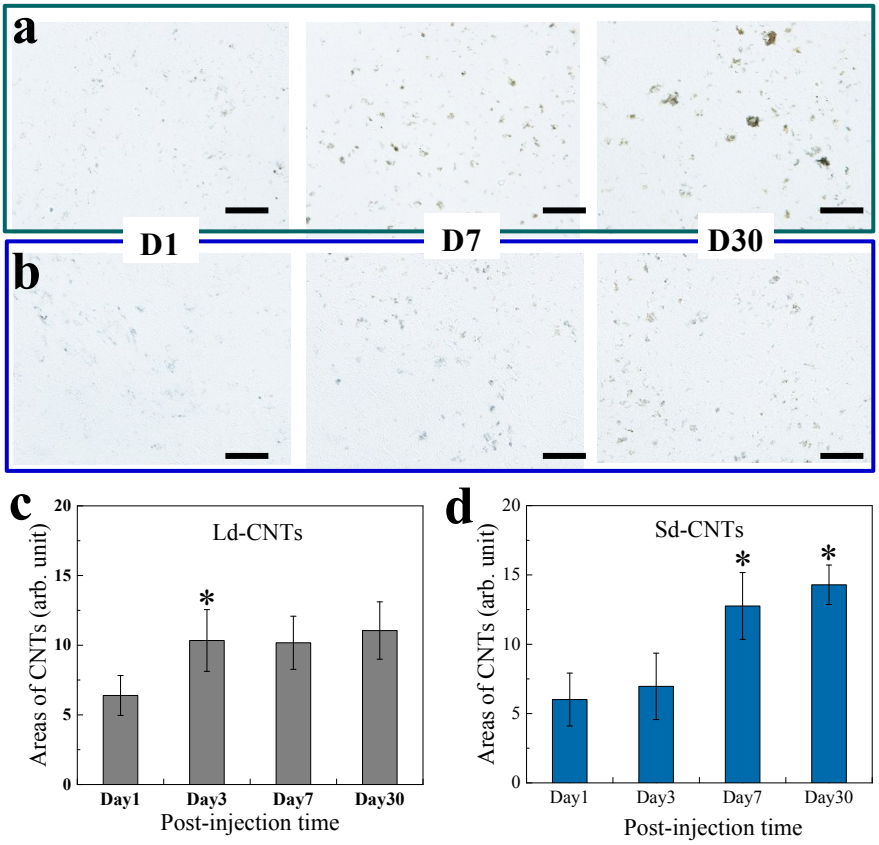

Figure SI-6. Optical microscopy images of unstained mouse spleens harvested at days (D)1, D7, and D30 after intravenous administration of a single dose of large-diameter carbon nanotubes (Ld-CNTs) (a) or small-diameter carbon nanotubes (Sd-CNTs) (b).Images of mouse livers after intravenous injection of Ld-CNTs and Sd-CNTs are shown as insets in (a) and (b), respectively. The average areas of the black spots in 20 images of tissues from mice injected with Ld-CNTs (c) or Sd-CNTs (d). Scale bar: 50 µm. *$p < 0.05$ and **$p < 0.01$ vs. the values at D1.

Figure SI-7

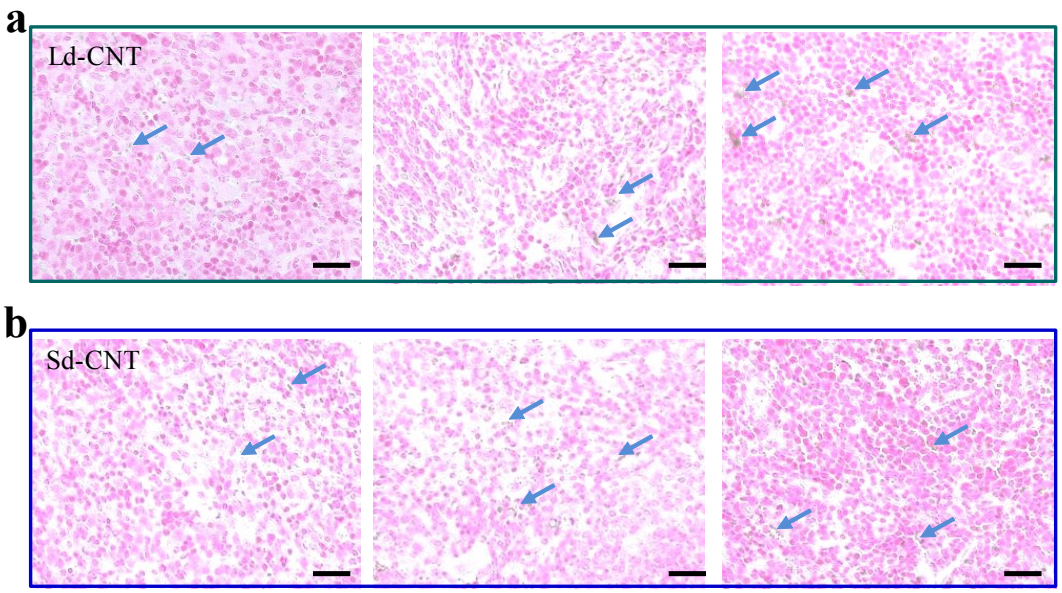

Figure SI-7. Optical microscopy images of nuclear fast red solution (kernechtrot) stained mouse spleens harvested at days (D)1, D7, and D30 after intravenous administration of a single dose of large-diameter carbon nanotubes (Ld-CNTs) (a) or small-diameter carbon nanotubes (Sd-CNTs) (b). Accumulated Ld-CNTs and Sd-CNTs are indicated by arrows. Scale bar: 25 μm.

Figure SI-8

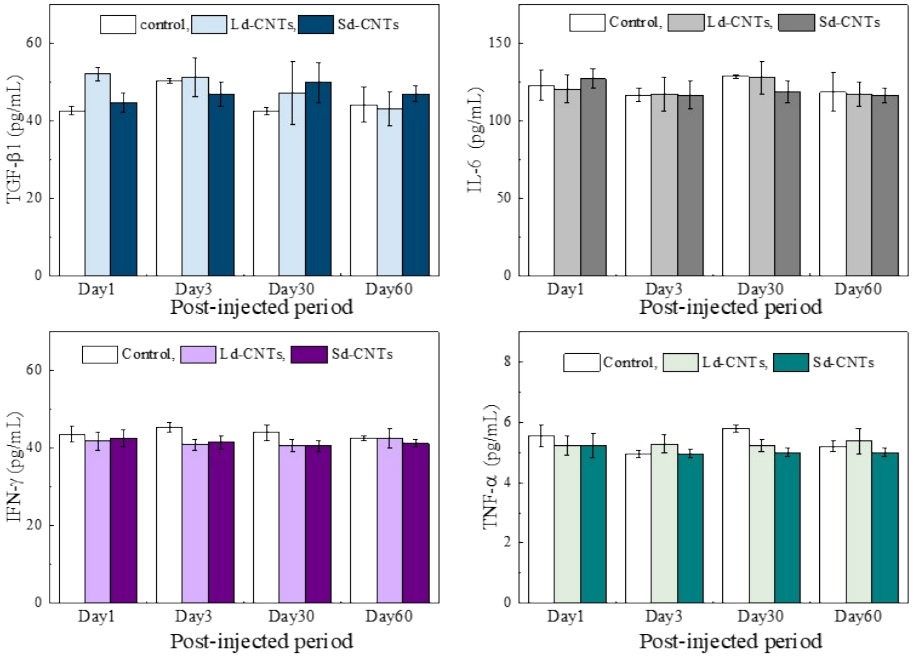

Figure SI-8. Concentrations of TGF-β1, IL-6, TNF-α, and INF-γ in lung lysates harvested 1, 3, 30, and 60 days after injection of Ld-CNTs or Sd-CNTs. Data are expressed as the mean ± SD (n = 5).

Figure SI-9

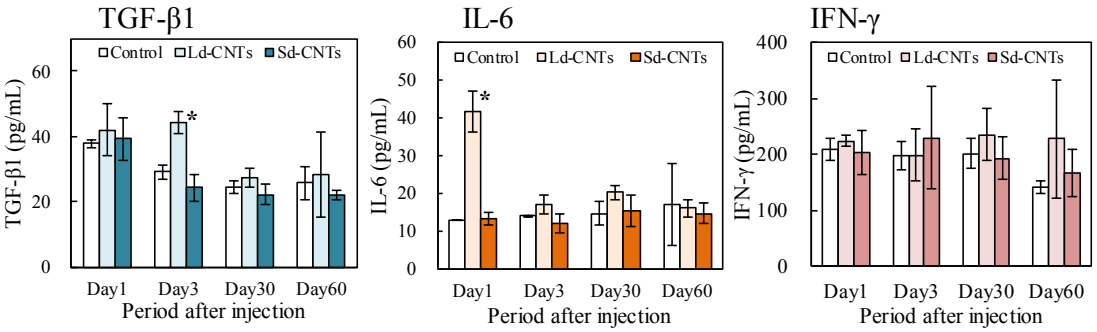

Figure SI-9. Concentrations of TGF-β1, IL-6, and INF-γ in liver lysates harvested 1, 3, 30, and 60 days after injection of Ld-CNTs or Sd-CNTs. Data are expressed as the mean ± SD (n = 5). *P<0.05 vs. the values of control.

Figure SI-10

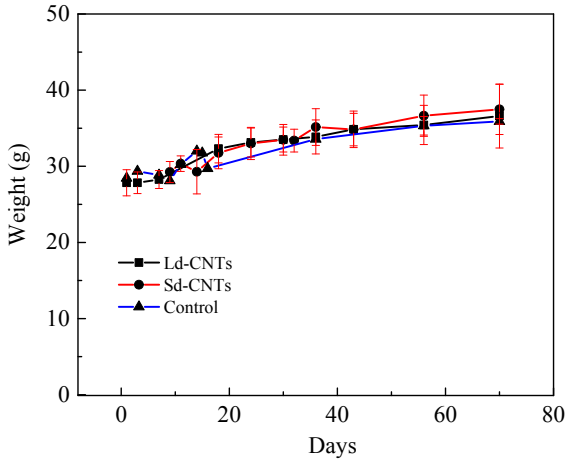

Figure SI-10. Body weights of mice after intravenous injection of PBS (control), Ld-CNTs, or Sd-CNTs. Data are expressed as the mean ± SD (n = 5). There was no significant difference between the three groups.

Figure SI-11

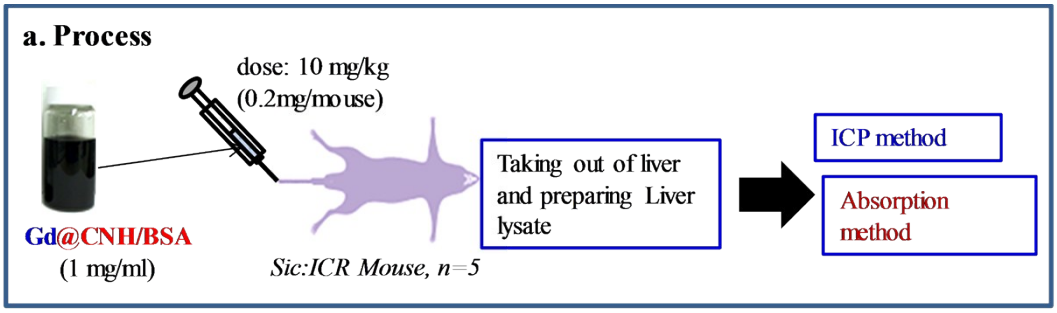

b. Result

		D1							D30						
	Mouse/ Liver	1	2	3	4	5	AV	SD	1	2	3	4	5	AV	SD
NIR absorption method	(μg/ml)	7.02	7.29	5.93	6.45	6.52	6.64	0.53	5.64	6.3	5.96	5.9	6.15	5.99	0.25
ICP method	(μg/ml)	6.63	6.1	5.84	6.1	6.63	6.26	0.33	5.84	5.84	6.1	6.1	5.57	5.89	0.15

Figure SI-11. Comparison of results obtained using elemental (Gd) analysis of ICP and the NIR optical absorption method. (a) Experiment design. (b) CNH quantities estimated by NIR light absorption and by ICP. The amounts of CNHs measured using two methods were similar at both time points (D1 and D30). The Gd@CNHs were obtained by incorporation of Gd_2O_3 into CNHs, as we reported previously [30].